

Galaxy Zoo: Dust and molecular gas in early-type galaxies with prominent dust lanes[†]

Sugata Kaviraj^{1,2*}, Yuan Sen Ting^{2,3}, Martin Bureau², Stanislav S. Shabala^{2,4}, R. Mark Crockett², Joseph Silk², Chris Lintott², Arfon Smith², William C. Keel⁵, Karen L. Masters⁶, Kevin Schawinski^{7,9} and Steven P. Bamford⁸

¹Blackett Laboratory, Imperial College London, London SW7 2AZ, UK

²Department of Physics, University of Oxford, Keble Road, Oxford, OX1 3RH, UK

³Ecole Polytechnique, 91128 Palaiseau Cedex, France

⁴School of Mathematics & Physics, Private Bag 37, University of Tasmania, Hobart 7001, Australia

⁵Department of Physics and Astronomy, 206 Gallalee Hall, 514 University Blvd., University of Alabama, Tuscaloosa, AL 35487-0234, USA

⁶Institute for Cosmology and Gravitation, University of Portsmouth, Dennis Sciama Building, Burnaby Road, Portsmouth PO1 3FX

⁷Department of Physics, Yale University, New Haven, CT 06511, USA

⁸School of Physics and Astronomy, University of Nottingham, University Park, Nottingham NG7 2RD

⁹Einstein Fellow

[†]This publication has been made possible by the participation of more than 250,000 volunteers in the Galaxy Zoo project. Their contributions are individually acknowledged at <http://www.galaxyzoo.org/Volunteers.aspx>.

25 February 2012

ABSTRACT

We explore the properties of dust and associated molecular gas in 352 nearby ($0.01 < z < 0.07$) early-type galaxies (ETGs) with prominent dust lanes, drawn from the *Sloan Digital Sky Survey*. Two-thirds of these ‘dusty ETGs’ (D-ETGs) are morphologically disturbed which suggests a merger origin, making these galaxies ideal testbeds for studying the merger process at low redshift. **The D-ETGs preferentially reside in lower-density environments, compared to a control sample drawn from the general ETG population.** Around 80% of D-ETGs inhabit the field (compared to 60% of the control ETGs) and less than 2% inhabit clusters (compared to 10% of the control ETGs). Compared to their control-sample counterparts, D-ETGs exhibit bluer UV-optical colours (indicating enhanced levels of star formation) and an AGN fraction that is more than an order of magnitude greater (**indicating a strikingly higher incidence of nuclear activity**). The mass of clumpy dust residing in large-scale dust features is estimated, using the SDSS *r*-band images, to be in the range $10^{4.5}$ to $10^{6.5} M_{\odot}$. A comparison to the total (clumpy + diffuse) dust masses - calculated using the far-infrared fluxes of the 15% of the D-ETGs that are detected by the *Infrared Astronomical Satellite* (*IRAS*) - indicates that only 20% of the dust is typically contained in these large-scale dust features. The dust masses are several times larger than the maximum value expected from stellar mass loss, ruling out an internal origin. The dust content shows no correlation with the blue luminosity, indicating that it is not related to a galactic-scale cooling flow. Furthermore, no correlation is found with the age of the recent starburst, suggesting that the dust is accreted directly in the merger rather than being produced in situ by the triggered star formation. Using molecular gas-to-dust ratios of ETGs in the literature we estimate that the median current molecular gas fraction in the *IRAS*-detected ETGs is $\sim 1.3\%$. Adopting reasonable values for gas depletion timescales and starburst ages, the median *initial* gas fraction in these D-ETGs is $\sim 4\%$. Recent work has suggested that the merger activity in nearby ETGs largely involves minor mergers (dry ETG + gas-rich dwarf), with mass ratios between 1:10 and 1:4. If the *IRAS*-detected D-ETGs have formed via this channel, then the original gas fractions of the accreted satellites are between 20 and 44%.

Key words: galaxies: ISM - galaxies: elliptical and lenticular, cD - galaxies: peculiar galaxies: interactions - galaxies: formation - galaxies: evolution

1 INTRODUCTION

As endpoints of the hierarchical buildup of mass, early-type galaxies (ETGs) possess a detailed fossil record of their progenitors. The stellar populations of ETGs encode the mass assembly history of galaxies over the lifetime of the Universe, and it is important that we gain a comprehensive understanding of their formation and evolution. While their red optical colours (e.g. Bower et al. 1992; Bernardi et al. 2003; Bell et al. 2004; Faber et al. 2007), high α -element enhancements (e.g. Thomas et al. 1999; Trager et al. 2000a,b) and obedience of a tight fundamental plane (e.g. Jorgensen et al. 1996; van Dokkum & Franx 1996; Saglia et al. 1997; Forbes et al. 1998) indicate that the bulk of their stellar populations ($> 80\%$) are old, the large scatter in the star-formation-sensitive ultraviolet (UV) colours of ETGs since $z \sim 1$ is interpreted as evidence for continuous low-level star formation at late epochs (Kaviraj et al. 2007, 2008; Martin et al. 2009, see also Fukugita et al. 2004; Yi et al. 2005; Jeong et al. 2007; Salim et al. 2010; Crockett et al. 2011). A coincidence between blue UV colours and morphological disturbances indicates that this star formation is merger-driven (Schweizer et al. 1990; Schweizer & Seitzer 1992; Kaviraj 2010; Kaviraj et al. 2011). Furthermore, the paucity of major mergers at late epochs (see e.g. Stewart et al. 2008; Jogee et al. 2009; López-Sanjuan et al. 2010) strongly suggests that the star formation is driven by *minor* mergers (Kaviraj et al. 2009, 2011). Our current understanding of ETG evolution therefore indicates that their underlying stellar populations are old, having been rapidly built at high redshift ($z > 1$), while the evolution at late epochs ($z < 1$) is dominated by repeated minor-merger events that contribute $< 20\%$ of their stellar mass at the present-day.

Notwithstanding the classical notion of ETGs being dry, passively-evolving systems, an extensive literature has developed over the past few decades on the inter-stellar medium (ISM) in these systems. The dust and gas content of *very* nearby ETGs has been studied by several authors (e.g. Tubbs 1980; Hawarden et al. 1981; Sadler & Gerhard 1985; Bertola 1987; Knapp et al. 1989; Goudfrooij & de Jong 1995; van Dokkum & Franx 1995; Knapp & Rupen 1996; Faber et al. 1997; Ebneter et al. 1988; Tomita et al. 2000; Tran et al. 2001; Combes et al. 2007; Calura et al. 2008; Young et al. 2011). While the galaxy samples and methodologies in these studies are varied, it is clear that the majority of ETGs in the very nearby Universe show evidence of dust (e.g. Knapp et al. 1989; van Dokkum & Franx 1995), the dust masses being generally inconsistent with scenarios in which the dust is supplied purely by stellar mass loss (e.g. Merluzzi 1998). Coupled with the frequently observed morphological disturbances and kinematical misalignments between gas and stars in these systems (e.g. Zeilinger et al. 1990; Sage & Galletta 1993; Annibali et al. 2010; Davis et al. 2011), it seems likely that a significant fraction of the inter-stellar matter has an external origin.

The accumulating evidence for widespread minor-merger-driven star formation (e.g. Kaviraj et al. 2009, 2011) makes the study of inter-stellar matter in ETGs all the more compelling. While the properties of the star formation have been quantified with a reasonable degree of precision, less is known about the fuel that drives this star formation. A study of the ISM of ETGs in modern observational surveys

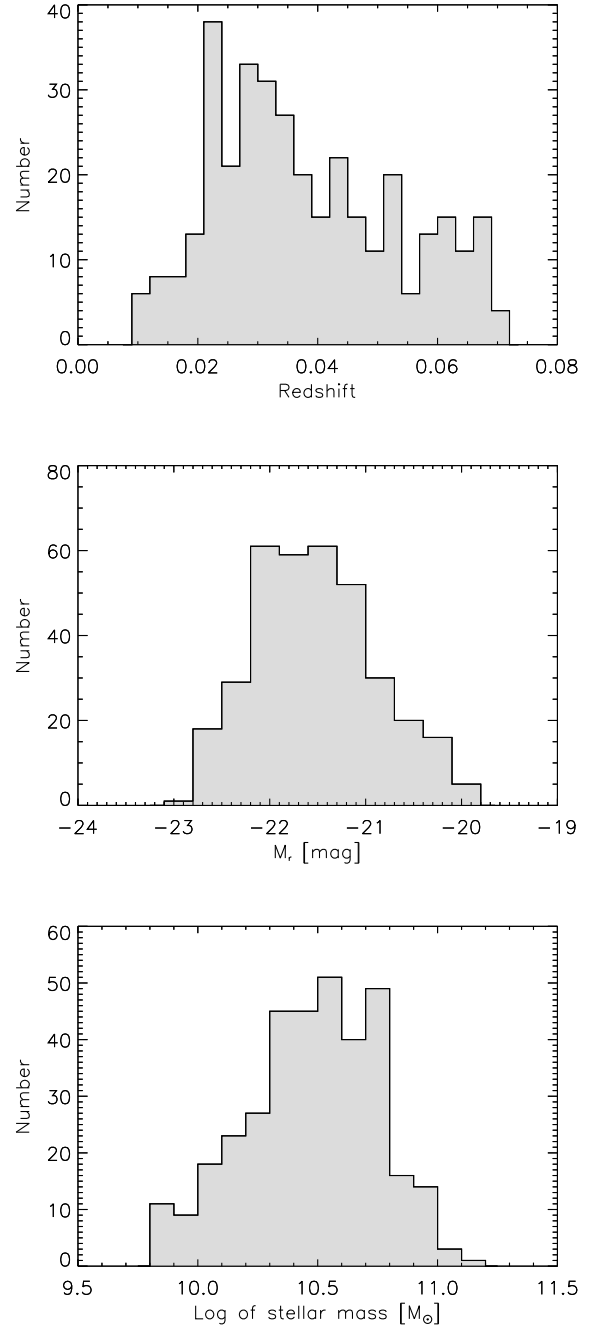


Figure 2. Distributions of redshift (top), r -band absolute magnitude (middle) and stellar mass (bottom) of the D-ETG sample in this study. As described in Section 2.2 below, the control samples to which these galaxies are compared are matched to the shape of the distributions presented here.

is therefore very desirable. In this paper we present a study of dusty ETGs (D-ETGs), drawn from Data Release 7 of the Sloan Digital Sky Survey (SDSS; Abazajian et al. 2009), that exhibit prominent, extended dust features in their optical images. In addition to exploring the properties of the dust, the homogeneous nature of the spectro-photometric data from the SDSS allows us to systematically study the star formation, active galactic nucleus (AGN) activity and

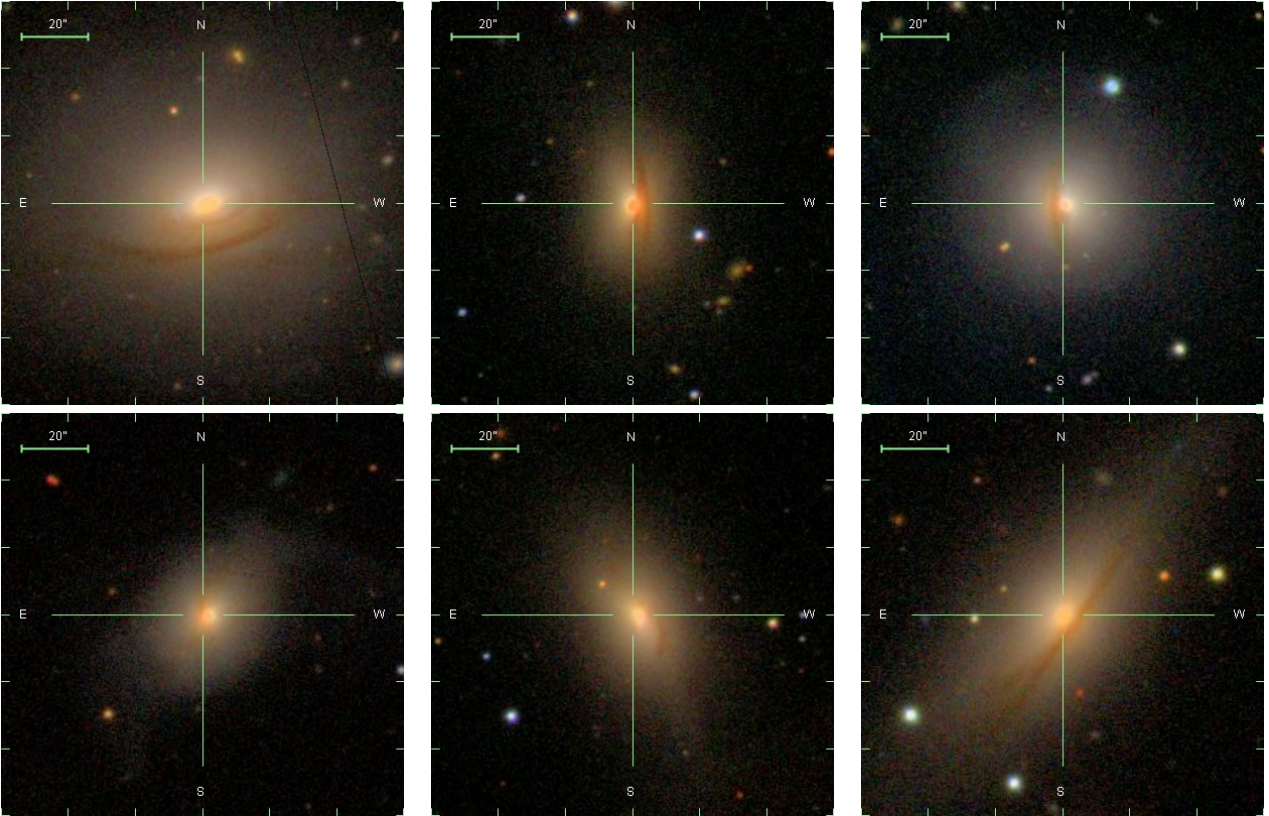


Figure 1. Examples of early-type galaxies with prominent dust features from the sample studied in this paper. Note the widespread morphological disturbances (shells and tidal tails) in the galaxies. A colour version of this figure is available in the online version of the journal.

local environment of the D-ETGs, compare these systems to a statistically meaningful ‘control’ sample drawn from the general ETG population and put some of the results in the literature on a firmer statistical footing. We are also able to explore the properties of the gas in the minor mergers that are responsible for star formation in nearby ETGs, and provide a more complete picture of the star formation activity in massive ETGs at late epochs.

The plan for this paper is as follows. Section 2 describes the selection of D-ETGs from the SDSS and the construction of a control sample to which their properties are compared. In Section 3 we discuss the high incidence of disturbed morphologies observed in the D-ETG sample. In Section 4 we explore the local environment of these galaxies and in Section 5 we employ UV-optical spectrophotometry to study their star formation and AGN activity. We explore the properties and origin of the dust in Section 6 and conclude by summarising our findings in Section 7.

2 DATA

2.1 Sample selection and basic properties

Galaxy Zoo (Lintott et al. 2008, 2010) is a citizen-science project that has used 250,000+ members of the general public to morphologically classify $\sim 900,000$ galaxies in the SDSS spectroscopic galaxy sample. The first incarnation of this project (Galaxy Zoo 1; GZ1) classified objects in the

SDSS galaxy population into broad morphological classes: early-types, spirals and mergers. Galaxy Zoo 2 (GZ2), an extension to GZ1 on which this study is based, has explored finer details of galaxy morphologies, such as morphological peculiarities (dust lanes, tidal disturbances, etc.) **Note that the GZ objects are taken from the SDSS GALAXY catalogue, which does not contain any quasars or Type I AGN. Broad-line objects are identified by a pipeline algorithm which compares the observed SDSS spectrum of individual galaxies to the composite spectrum of (Vanden Berk et al. 2001)¹.**

Around 19,000 GZ2 galaxies in the redshift range $0.01 < z < 0.1$ are flagged as containing a dust feature by *at least one* GZ2 user. Each galaxy in this sample was visually re-inspected by SK and YST to determine (1) whether the galaxy really has a dust feature (2) the morphology of the parent galaxy (ETG or non-ETG) and (3) whether the galaxy is morphologically disturbed. After this second layer of visual inspection we decided to restrict this study to the redshift range $z < 0.07$, because the unambiguous detection of a dust feature appears to become difficult beyond this redshift. **Note that the identification of D-ETGs is not expected to be dependent on galaxy luminosity. As long as the dust is backlit by the galaxy it is readily visible.** This process yields a final sample of reliably classified 352 D-ETGs, which are the subject of this paper. They represent 4% of the ETG

¹ http://www.sdss.org/dr7/algorithms/redshift_type.html

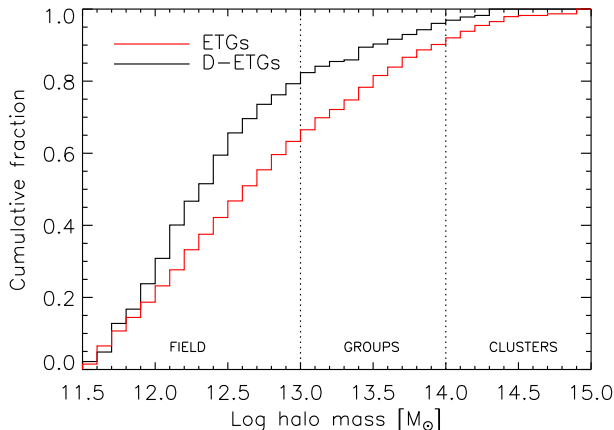


Figure 3. Cumulative distribution of host dark matter halo masses for D-ETGs and the ETG control sample. Compared to the control sample, D-ETGs preferentially inhabit lower density environments. Almost 80% of the D-ETGs reside in the field (compared to 60% of the control ETG population) and less than 2% of the D-ETGs reside in clusters (compared to 10% of their control-sample counterparts). A colour version of this figure is available in the online version of the journal.

population (restricted to the same redshift and magnitude ranges as the D-ETG sample).

Figure 1 shows several typical examples of our D-ETGs. Figure 2 shows the basic properties of the D-ETG sample: the redshift, absolute r -band magnitude and stellar mass distributions. Stellar masses are calculated using the calibrations of Bell et al. (2003). All magnitudes shown in this paper have been K-corrected, using the latest version of the public KCORRECT code (Blanton et al. 2003; Blanton & Roweis 2007).

2.2 Control sample

An important objective of this paper is a systematic comparison between the properties of D-ETGs and those of a control sample of galaxies from the general ETG population. We create a control sample of ~ 4000 ETGs, using galaxies from GZ2 which have an early-type ‘vote fraction’ greater than 0.7, i.e. more than 70% of the users that classified each of these objects flagged it as an ETG. **The control sample is selected to be ‘dustless’ i.e. no GZ user flagged any of these galaxies as having a dustlane. The control sample is then visually inspected to remove late-type contaminants (the contamination rate is very low, around 3%) and flag control ETGs that have morphological disturbances.** The control sample is further constructed so that it has the same redshift and magnitude distributions as the D-ETG population shown in Figure 2.

3 DISTURBED MORPHOLOGIES: A MERGER ORIGIN FOR DUSTY ETGS

The visual inspection described above indicates that $\sim 65\%$ of D-ETGs show clear morphological disturbances, at the depth of the standard SDSS images. In comparison, the

control sample (described in Section 2.2 above) shows a disturbed fraction of only around 6%. The fraction of disturbed objects in the D-ETG sample is therefore strikingly high, indicating that D-ETGs are the products of recent interaction events and, in agreement with the literature (e.g. Goudfrooij et al. 1994a), that the formation of the dust is likely to be the result of these interactions. Indeed the D-ETGs in this sample are likely to represent objects like Centaurus A *in the making* and are thus ideal testbeds for studying the merger process in the low-redshift Universe.

4 LOCAL ENVIRONMENT

We begin by probing the local environment of our D-ETGs, by cross-matching this sample with the SDSS environment catalogue constructed by Yang et al. (2007, 2008), who use a halo-based group finder to separate the SDSS into over 300,000 structures with a broad dynamic range, from rich clusters to isolated galaxies. This catalogue provides estimates of the masses of the host dark matter (DM) haloes of individual SDSS galaxies, which are related to the traditional classifications of environment (‘field’, ‘group’ and ‘cluster’). Cluster-sized haloes typically have masses greater than $10^{14} M_{\odot}$, while group-sized haloes have masses between 10^{13} and $10^{14} M_{\odot}$. Smaller DM haloes constitute what is commonly termed the field.

In Figure 3 we present the cumulative distribution of host DM halo mass for both the D-ETGs and the ETG control sample. We find that, compared to the control ETG population, D-ETGs preferentially inhabit lower-density environments. Almost 80% of D-ETGs reside in the field (compared to 60% of the control ETGs) and less than 2% reside in clusters (compared to 10% of their control-sample counterparts). This is consistent with the idea that the D-ETGs are merger remnants, since the high relative velocities in cluster environments make mergers unlikely (Binney & Tremaine 1987).

5 STAR FORMATION AND AGN ACTIVITY

Figure 4 shows the $(g-r)$ and $(NUV-r)$ colour distributions of the D-ETGs compared to those of their control-sample counterparts. The optical g and r magnitudes are taken from the SDSS (York et al. 2000). The NUV magnitudes are from the *Galaxy Evolution Explorer (GALEX)* space telescope (Martin et al. 2005). The GALEX NUV filter is centred at $\sim 2300 \text{ \AA}$ (Morrissey et al. 2007). We use the recommended total magnitudes in the AB systems for both the SDSS and GALEX photometry (Stoughton et al. 2002; Morrissey et al. 2007).

We find that the D-ETGs are redder than their control counterparts in the optical $(g-r)$ colour, which is consistent with the visibly high levels of dust present in these systems. Nevertheless, the D-ETG population is bluer than the control sample in the $(NUV-r)$ colour, with a median offset of ~ 0.5 mag. Given that the UV wavelengths are several times more sensitive to young stars than the optical wavelengths (see e.g. Figure 1 in Kaviraj et al. 2009), the bluer UV-optical colours are likely to be driven by recent or ongoing star formation in the D-ETG population. It is important

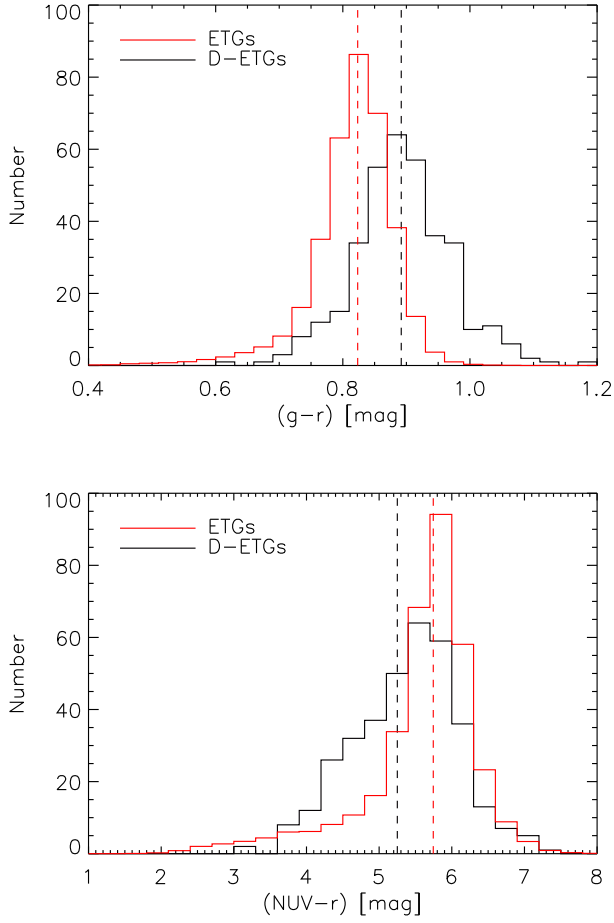


Figure 4. TOP: Optical $(g-r)$ colour distributions of the D-ETGs and the control ETGs. Unsurprisingly, the D-ETGs are found to be redder than their control counterparts, due to the presence of visibly large amounts of dust. **BOTTOM:** $(NUV-r)$ colour distributions of the D-ETGs and the control ETGs. The D-ETGs are bluer in the UV-optical colour, presumably due to recent star formation (see text for details). Median values are shown using the dashed vertical lines. A colour version of this figure is available in the online version of the journal.

to note that the large-scale structure of the dust in the D-ETGs is clumpy and does not entirely obscure the galaxy core (see Figure 1), where the young stars (which dominate the UV flux) are typically concentrated (e.g. Ferreras et al. 2009; Jeong et al. 2009; Suh et al. 2010; Peirani et al. 2010).

We proceed by probing the dominant gas ionisation mechanism in the D-ETG sample. The presence of dust implies the availability of gas which, in turn, makes the presence of star formation and nuclear activity in these galaxies likely. We use a standard optical emission-line ratio analysis (Kewley et al. 2006, see also Baldwin et al. 1981, Veilleux et al. 1987, Kauffmann et al. 2003) which exploits the $[\text{NII}]/\text{H}\alpha$ and $[\text{OIII}]/\text{H}\beta$ ratios to probe the presence of Type II AGN in our D-ETG sample. The optical emission-line fluxes are calculated from the SDSS spectrum of each object using the public GANDALF code (Sarzi et al. 2006). Note that the SDSS spectra are measured in $3''$ fibres (~ 4 kpc at $z = 0.035$, the median redshift of our D-ETG sample) centred on the

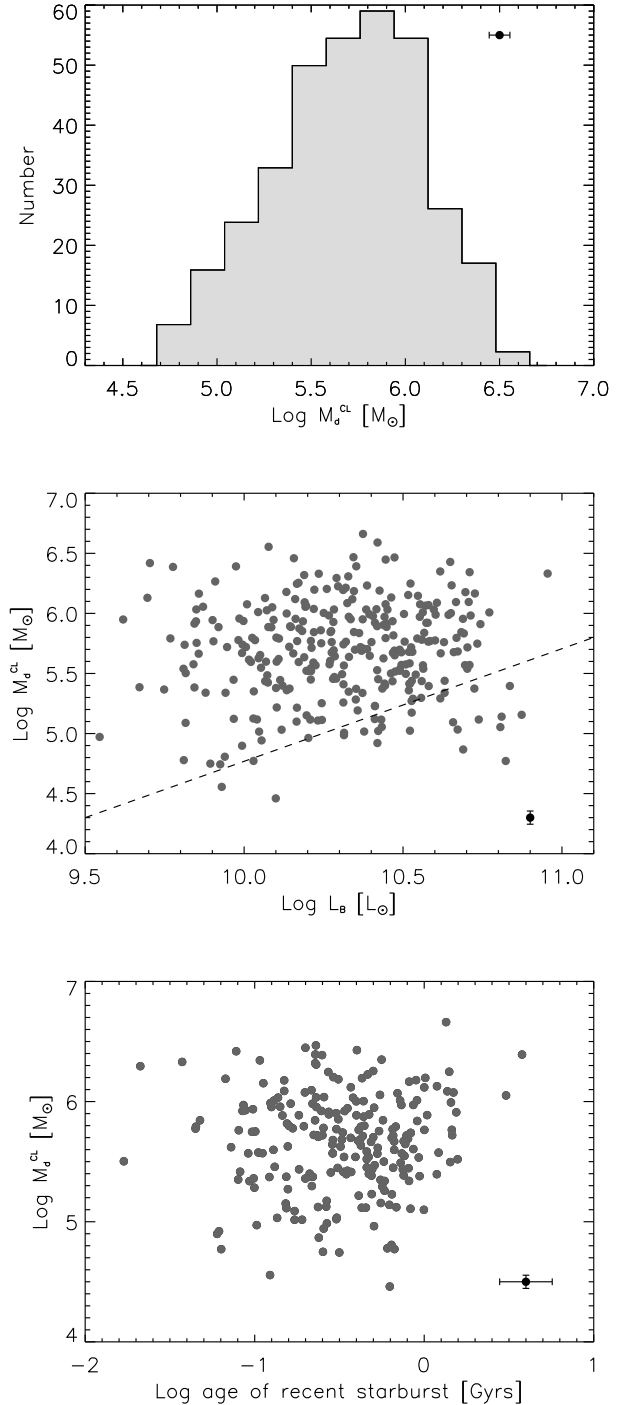


Figure 5. TOP: Distribution of clumpy dust mass (M_d^{CL}) in the D-ETGs, derived from their optical r -band images (see text for details). **MIDDLE:** Clumpy dust mass vs. blue luminosity of the D-ETGs. **BOTTOM:** Clumpy dust mass vs. age of the recent starburst, estimated from UV-optical colours. Note that, while the formal error on M_d^{CL} is ~ 0.055 dex (driven by the uncertainties in A_V), the uncertainties in the assumed dust distribution induces an additional error of up to 0.3 dex (see text for details).

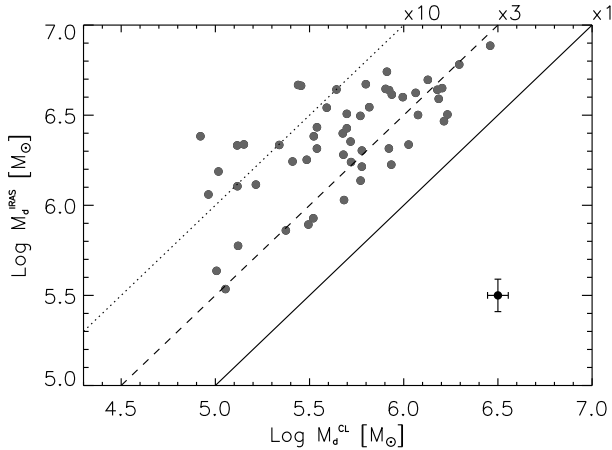


Figure 6. Comparison of the clumpy dust masses (M_d^{CL}), derived from the optical r -band images, with the dust masses derived from *IRAS* fluxes M_d^{IRAS} . The *IRAS*-derived dust masses are typically a factor of 4.5 larger than their clumpy counterparts. **Note that the error bar in M_d^{IRAS} is the error from Eqn 3.**

galaxy. Galaxies in which all four emission lines are detected with a signal-to-noise ratio greater than 3 are classified as either ‘star-forming’, ‘composite’ (i.e. hosting both star formation and AGN activity), ‘Seyfert’ or ‘LINER’. Galaxies without a detection in all four lines are classified as ‘quiescent’. The fraction of galaxies in each emission-line class is listed in Table 1, for both the D-ETG and control samples.

We find that the fractions of D-ETGs classified as star-forming and composite are factors of 3 and 8 larger respectively than that for the control ETGs. This suggests enhanced levels of star formation in the D-ETG population compared to its control counterpart, consistent with the UV-optical colour analysis above. The fraction of LINERS in the D-ETGs is also greater by a factor of 3, plausibly due to LINER-like emission from merger-driven shocks or evolved stellar populations (such as post-asymptotic giant branch stars) that are associated with the star formation (e.g. Sarzi et al. 2010). Table 1 indicates that, in addition to enhanced star formation and LINER emission, the D-ETGs exhibit a strikingly higher Seyfert fraction, more than an order of magnitude larger than in their control-sample counterparts. The fraction of quiescent galaxies is correspondingly an order of magnitude smaller. Therefore, the presence of prominent dust features in an ETG significantly increases its chances of hosting both more star formation and more nuclear activity, with nuclear activity being the dominant gas ionisation mechanism in these systems.

6 PROPERTIES OF THE DUST AND ASSOCIATED GAS

6.1 Clumpy dust

The dust in D-ETGs is comprised of both clumpy structures, that are easily visible in the optical images, and diffuse dust, that is intermixed with the stars and is essentially invisible in the optical imaging. We begin by calculating the dust contained within the clumpy features (M_d^{CL}), following a

Table 1. Comparison of star formation and AGN activity, derived using optical emission-line-ratio diagnostics, in the D-ETGs and their control-sample counterparts.

	D-ETGs	Control ETGs	f(D-ETG)/f(Ctrl)
Star-forming	7.2%	2.1%	3.4
Composite	22.8%	2.8%	8.1
Seyfert	19.9%	1.7%	11.7
LINER	37.5%	10.4%	3.6
Quiescent	12.8%	83.0%	0.2

method similar to that employed by several previous studies (e.g. Sadler & Gerhard 1985; van Dokkum & Franx 1995; Tran et al. 2001). The clumpy dust mass is given by

$$M_d^{\text{CL}} = \langle A_V \rangle \Sigma \Gamma_V^{-1}, \quad (1)$$

where $\langle A_V \rangle$ is the mean V -band extinction in magnitudes, Σ is the total area of the dust features and Γ_V is the mass absorption coefficient².

Following these previous studies, A_V is measured as follows. Ellipses are first fitted to the isophotes of the SDSS r -band images of each galaxy, using the IRAF task ELLIPSE, with the dust features masked out. An absorption map is then created, using the ratio of the flux in the observed image (F_{obs}) to the flux in the model fit (F_{mod}). The optical depth is $\tau = -\ln(F_{\text{obs}}/F_{\text{mod}})$ and $A_r = 1.09\tau$ (Tran et al. 2001). We convert A_r to A_V using the Galactic dust law: $A_V = 1.33A_r$ (Tran et al. 2001). **Note that the quality of the fits are unaffected by the faint tidal features that are found on the outskirts of the D-ETGs.**

Several studies have shown that the extinction curves in ETGs with dust lanes are similar to their Galactic counterpart (see e.g. Sadler & Gerhard 1985; Goudfrooij et al. 1994a; Sahu et al. 1998; Finkelman et al. 2008), which indicates that the properties of the dust in these systems are similar to that in the Galaxy. Therefore, it appears reasonable to employ the Galactic value for the mass absorption coefficient (i.e. $\Gamma_V = 6 \times 10^{-6} \text{ mag kpc}^2 M_\odot^{-1}$) although we note that a more accurate calculation requires a measurement of Γ_V in our individual D-ETGs. The formal error on M_d^{CL} (driven, in this case, only by the error in $\langle A_V \rangle$) is calculated using the standard error propagation formula. We note that the errors in other quantities that appear later in this study (e.g. M_d^{IRAS} and g_i) are also calculated using the standard error formula.

While the formal error on M_d^{CL} is only ~ 0.055 dex, this derivation assumes that the dust is placed in a simple foreground screen in front of the light source, while in actual fact the dust is embedded in the galaxy. The use of this simplifying assumption induces an additional uncertainty of up to ~ 0.3 dex in the dust mass calculation (e.g. Tomita et al. 2000; Tran et al. 2001). The values derived here (see the top panel of Figure 5) are in the range $10^{4.5}$ to $10^{6.5} M_\odot$,

² The right-hand side of Eqn 1 is derived as follows. If δ is the area of a single pixel and A_i is the extinction in pixel i then: $M_d^{\text{CL}} = [\delta A_1 + \delta A_2 + \delta A_3 + \dots + \delta A_n] \Gamma_V^{-1}$. Since the total area $\Sigma \equiv n\delta$, $M_d^{\text{CL}} = (\Sigma/n)[A_1 + A_2 + A_3 + \dots + A_n] \Gamma_V^{-1} = \langle A \rangle \Sigma \Gamma_V^{-1}$.

in good agreement with the range of clumpy dust masses derived using similar techniques in the literature (10^3 - $10^7 M_\odot$; Sadler & Gerhard 1985; van Dokkum & Franx 1995; Goudfrooij & de Jong 1995; Tomita et al. 2000; Tran et al. 2001; Whitaker & van Dokkum 2008).

In the middle panel of Figure 5, we plot the clumpy dust mass of the D-ETGs against their total blue luminosity (L_B). L_B is calculated from the absolute (total) B -band magnitude, after transforming from the absolute SDSS (total) g -band magnitude using the relation $m_B = m_g + 0.3$ (Rodgers et al. 2006). We use L_B to facilitate direct comparison with previous studies (e.g. Merluzzi 1998). The dashed line indicates the maximum expected contribution to the dust content from stellar mass loss alone (e.g. Faber & Gallagher 1976; Knapp et al. 1992), assuming that the dust is depleted by sputtering (e.g. Spitzer 1978; Draine & Salpeter 1979a,b; Dwek 1986; Dwek et al. 1990) over a maximal destruction timescale of $\sim 10^{7.5}$ years (Faber & Gallagher 1976). In agreement with previous studies (e.g. Goudfrooij et al. 1994b; Merluzzi 1998), we find that (1) D-ETGs typically have clumpy dust masses that are well in excess of the maximum equilibrium mass expected from stellar mass loss alone and (2) there is no correlation between the optical dust masses and L_B . It is worth noting that L_B shows a correlation with the total X-ray luminosity (L_X) of ETGs, which traces their hot gas content (e.g. Canizares et al. 1987; Mathews & Brighenti 2003; Mulchaey & Jeltama 2010). The lack of a correlation between the clumpy dust mass and L_B suggests that the clumpy dust is not produced through cooling from the hot gas reservoirs that may be present in these ETGs (see also Forbes 1991; Bregman et al. 1992). Recall also that the D-ETGs studied in this paper do not typically inhabit clusters, so that cluster-scale cooling flows are not relevant to these systems.

The dust properties derived above indicate that the clumpy dust content of the D-ETGs is not created by internal processes such as stellar mass loss or gas cooling. Together with the high incidence of morphological disturbances observed in the D-ETG sample (see Section 3), this indicates that the clumpy dust observed in these galaxies is likely to be associated with the recent merger events that created these objects.

Since star formation is clearly enhanced in D-ETGs, it is worth exploring whether the dust is produced in situ by this star formation or whether it is directly accreted in the mergers. In the bottom panel of Figure 5 we plot the clumpy dust mass of D-ETGs against the age of the recent starburst (T), which has been estimated using the UV-optical colour (see Section 4.2.1 and 4.3 in Kaviraj 2010):

$$\log T [\text{Gyrs}] \sim 0.6^{\pm 0.03} \times [(NUV - u) - (g - z) - 1.73^{\pm 0.03}]. \quad (2)$$

Briefly, (see Sections 4.2.1 and 4.3 in Kaviraj 2010 for details), T is one of several star formation history (SFH) parameters derived for individual ETGs by fitting their GALEX/SDSS UV-optical photometry to a library of synthetic photometry, generated using a large collection of model SFHs. The model SFHs assume two instantaneous bursts, the first fixed at $z = 3$ (since the bulk of the stars in ETGs are old), while the second (which represents the recent star formation episode) is allowed to vary in age

(T) and mass fraction (realistic ranges of dust and metallicity are applied to the model SFHs). Kaviraj (2010) extract marginalised values for the free parameters including T and find a strong correlation between the marginalised values of T and the relatively dust-insensitive double colour $[(NUV - u) - (g - z)]$. This relation (Eqn 2) allows us to estimate the age of the recent starburst in ETGs from the observed value of $[(NUV - u) - (g - z)]$.

Figure 5 shows that the clumpy dust mass does not correlate with T . The apparent decoupling between the age of the recent (merger-induced) star formation episode and the clumpy dust content in D-ETGs favours a scenario in which the dust is directly accreted during the merger and not created in situ by the triggered star formation.

6.2 Diffuse dust and the total dust content

Since the diffuse dust mass in the ISM cannot be estimated from the optical images, the clumpy dust masses calculated above are *likely to be lower limits* to the total dust masses. It is thus desirable to quantify the total (diffuse + clumpy) dust content of these systems, at least to gain an understanding of how much dust is not contained in the clumpy features visible in the optical images. A useful route to estimating the total dust content is to use the far-infrared spectrum. Around 15% of our D-ETGs have infrared data from the *Infrared Astronomical Satellite (IRAS)*, which we use to estimate the ‘total’ dust mass in these galaxies. It should be noted, however, that *IRAS* is insensitive to very cold dust, with a temperature less than ~ 20 K (e.g. Henkel & Wiklind 1997). Thus, while the *IRAS* fluxes are a much better estimator of the total dust mass than the optical images, more accurate estimates require imaging by new instruments such as *Herschel*, that probe the far-infrared spectrum beyond $100 \mu\text{m}$.

Following past studies (e.g. Goudfrooij & de Jong 1995; Tran et al. 2001), the *IRAS*-derived dust masses (M_d^{IRAS}) are calculated using the formula (see e.g. Schwartz 1982; Hildebrand 1983; Rowan-Robinson 1986; Kwan & Xie 1992)

$$M_d^{\text{IRAS}} = 5.1 \times 10^{-11} S_\nu D^2 \lambda_\nu^4 [e^{(1.44 \times 10^4 / \lambda_\nu T_d)} - 1] M_\odot, \quad (3)$$

where the dust temperature (T_d) is estimated using the *IRAS* flux ratio S_{60}/S_{100} and an emissivity law that varies as λ^{-1} , S_ν is the *IRAS* flux density in mJy at wavelength ν , D is distance to the galaxy in Mpc and λ_ν is the wavelength in microns. We use $\nu = 100 \mu\text{m}$ for our calculations. Figure 6 shows the *IRAS*-derived dust masses plotted against the clumpy dust masses, for the subset of D-ETGs that have *IRAS* detections at 60 and $100 \mu\text{m}$. The *IRAS* fluxes are taken from the *Imperial IRAS-FSC Redshift Catalogue* (Wang & Rowan-Robinson 2009). The median discrepancy between the clumpy dust mass and the *IRAS* dust mass is a factor of 4.5. In other words, only $\sim 20\%$ of the dust is typically contained in clumpy features. Nevertheless, the *IRAS* dust masses show the same lack of correlation with blue luminosity and starburst age as do the clumpy dust masses, leaving our conclusions above unchanged.

6.3 Cold molecular gas

Given the close correspondence between dust and cold gas (e.g. Knapp 1999), it is instructive to explore the properties of the cold gas reservoirs of our D-ETGs. We choose to focus on *molecular* gas (i.e. H_2 , derived from CO observations) because of its relevance to star formation (e.g. Wong & Blitz 2002; Schaye 2004; Krumholz & McKee 2005; Leroy et al. 2008) and the better availability of *molecular gas data* on ETGs in the literature compared to its atomic counterpart (HI). We note first that previous studies have typically assumed that the molecular gas-to-dust (G/D) ratios in ETGs are similar to that in the Galaxy (~ 150 ; see e.g. Spitzer 1978; Hildebrand 1983; Draine & Lee 1984). However, if the dust is directly accreted during recent mergers (c.f. Section 6.1), then the Galactic G/D ratio is inappropriate for all ETGs, unless the accreted companions are all Milky-Way-like. In fact, recent work (e.g. Kaviraj et al. 2009, 2011; Crockett et al. 2011) has shown that a large proportion of the merger activity experienced by nearby ETGs involves interactions with small gas-rich companions (rather than Milky Way-like systems), implying that the Galactic G/D value may not be appropriate for our D-ETG sample.

To obtain a more realistic conversion between dust and molecular gas for our D-ETGs, we appeal to measurements of molecular G/D ratios in ETGs that are available in the literature. For 76 ETGs studied by Wiklind & Henkel (1989), Thronson et al. (1989), Gordon (1991), Lees et al. (1991), Wang et al. (1992) and Wiklind & Henkel (1995), the average molecular G/D ratio is 1190 ± 410 . Thus, the molecular G/D values appropriate for our D-ETGs are likely to be almost an order of magnitude higher than the value in the Galaxy. We note here that the measured G/D ratios in ETGs are indeed around the values typical of late-type dwarfs (e.g. Young et al. 1989), further supporting the view that the interactions that produce the D-ETGs probably involve the accretion of gas-rich satellites. In the top panel of Figure 7, we use the *IRAS* dust masses to estimate the current molecular gas contents, assuming a G/D ratio of 1190 ± 410 . The median molecular gas fraction (i.e. molecular gas mass divided by stellar mass) is $\sim 1.3\%$. The error bars incorporate both the uncertainty on the G/D value and the errors in the *IRAS*-derived dust masses. It is worth noting that this value is well within the distribution of molecular gas fractions found by Young et al. (2011) in a volume-limited sample of *normal* ETGs in the ATLAS^{3D} survey of very nearby ETGs.

Since star formation is ongoing in these galaxies, we expect the current molecular gas masses calculated above to be lower than the initial molecular gas contents. Given a characteristic exponential timescale (τ_d) for the gas depletion (which is also the star formation timescale), the current molecular gas fraction (g_0) is related to the initial value (g_i) by

$$g_0 = g_i e^{(-T/\tau_d)}, \quad (4)$$

where T is the look-back time to the onset of star formation (i.e. the starburst age). Using Eqn 2 to estimate T , and adopting a value of 0.1 Gyr for the characteristic timescale of the recent star formation episodes in ETGs (see Schawinski et al. 2007), we estimate g_i in each of our D-ETGs.

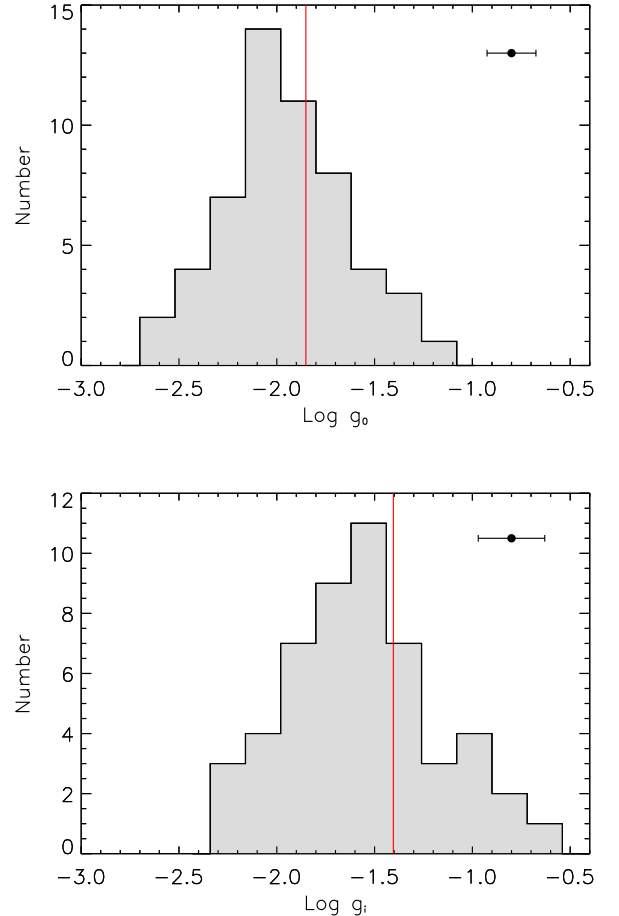


Figure 7. Derived current (top) and initial (bottom) molecular gas fractions (i.e. molecular gas mass divided by the stellar mass) in the subset of D-ETGs that are detected by *IRAS* (see text for details). Median values of the distributions are indicated using solid (red) lines.

These initial molecular gas fractions are presented in the bottom panel of Figure 7. The estimated initial gas fractions are small, with a median value of around 4%. Recent work (see e.g. Kaviraj et al. 2009, 2011) has suggested that the merger activity (and associated star formation) in nearby ETGs largely involves minor mergers between dry ETGs and gas-rich satellites with mass ratios between 1:4 and 1:10. If the *IRAS*-detected D-ETGs indeed formed via this channel, then a typical initial gas fraction of 4% implies that the gas fractions of the accreted satellites are likely to be between $\sim 20\%$ and $\sim 44\%$ (assuming that the ETGs themselves are gas-free). It is worth noting that these empirical results are consistent with recent numerical work which suggests that the satellites fuelling the star formation in nearby ETGs should have molecular gas fractions greater than 20% (Kaviraj et al. 2009). It should also be noted that the molecular gas analysis is only representative of the 15% of D-ETGs that are detected by *IRAS*. A more robust statistical analysis requires infrared data on the entirety of the D-ETG sample studied here.

7 SUMMARY

We have explored the properties of dust and associated molecular gas in ETGs, by studying 352 nearby ($0.01 < z < 0.07$) ETGs with prominent dust features in the SDSS DR7. The galaxies were identified through direct visual inspection of SDSS images using the Galaxy Zoo 2 project. Our analysis has focussed on comparing the local environment, star formation and nuclear activity of these dusty ETGs (D-ETGs) to those of a control sample drawn from the general ETG population. We have then explored the properties and origin of the dust and associated molecular gas in these systems, and studied the processes that lead to their formation.

Two-thirds of the D-ETGs show morphological disturbances at the depth of the standard SDSS images, suggesting a merger origin for these galaxies. D-ETGs reside preferentially in low-density environments, with 80% inhabiting the field (compared to 60% of their control-sample counterparts) and less than 2% inhabiting clusters (compared to 10% of their control-sample counterparts). D-ETGs show bluer UV-optical colours compared to the control ETG population, indicating the presence of enhanced levels of star formation activity. An analysis using optical emission-line ratios indicates that the fraction of objects classified as star-forming and composite are factors of 3 and 8 higher respectively in the D-ETGs compared to their control-sample counterparts. The fraction of Seyferts is more than an order of magnitude higher, while the fraction of galaxies classified as quiescent is correspondingly an order of magnitude smaller in the D-ETG population compared to that in the control sample. The presence of prominent dust features in an ETG therefore significantly increases its chances of hosting both star formation and nuclear activity, with nuclear activity being the dominant gas ionisation mechanism.

We have explored the dust content of our D-ETGs, both in terms of the clumpy dust mass contained in the large-scale dust features (visible in the optical SDSS images), and in terms of the diffuse dust that may exist in the ISM. The clumpy dust masses span the range $10^{4.5}$ to $10^{6.5} M_{\odot}$ and are typically several factors higher than the maximum dust contribution expected from stellar mass loss from the old, underlying stellar populations that dominate ETGs. The clumpy dust mass does not correlate with the blue luminosity of the galaxies, indicating that galactic-scale cooling flows are unlikely to be responsible for the dust content. Similarly, no correlation is found between the clumpy dust content and the age of the recent starburst, suggesting that the dust is not produced in situ from the star formation triggered by the merger event, but is rather accreted directly during the merger.

The clumpy dust masses are strictly lower limits to the total dust masses because they not include diffuse dust which may be intermixed with the stars and is essentially invisible in the optical images. In the 15% of our D-ETGs that are detected by *IRAS*, we have estimated the ‘total’ (clumpy + diffuse) dust mass using the *IRAS* 60 and 100 μm fluxes. The average discrepancy between the clumpy and *IRAS*-derived dust mass in these D-ETGs is a factor of 4.5. In other words, only $\sim 20\%$ of the dust mass in these objects is contained in the large-scale dust features that are observed in the optical images. Nevertheless, the *IRAS* dust masses

show the same lack of correlation with galaxy properties and starburst ages as their clumpy counterparts.

The correspondence between dust and cold gas allows us to explore the properties of the cold gas reservoirs in our D-ETGs. Restricting ourselves to the *IRAS*-detected galaxies (in which we have a reasonable estimates of the total dust mass), we employ the average molecular gas-to-dust ratio of ETGs in the literature (~ 1190) to estimate the current molecular gas fractions of these objects. The median value of the current gas fraction is $\sim 1.3\%$. Given the current molecular gas fraction, an estimate of the age of the starburst and a characteristic gas depletion (star formation) timescale, we have estimated the *initial* molecular gas fraction in each *IRAS*-detected D-ETG, with a median value of $\sim 4\%$. Given recent work that suggests that the merger activity in nearby ETGs largely involves minor mergers with mass ratios between 1:10 and 1:4 (e.g. Kaviraj et al. 2009), a typical initial molecular gas fraction of 4% suggests that the gas-rich satellites accreted by the *IRAS*-detected ETGs are likely to have had molecular gas fractions between ~ 20 and 44% (assuming that the ETGs themselves are gas and dust-free).

While recent UV-optical studies have measured the continuous (minor-merger-driven) star formation in ETGs over the last 8 billion years, less is known about the dust and associated gas that drives this star formation. This paper has offered insights into the inter-stellar medium of nearby ETGs that are merger remnants and, in particular, the initial gas masses plausibly brought in by the satellites that drive the star formation. **The galaxy sample studied here provides an ideal basis for future studies of D-ETGs using new instruments such as *Herschel* and the *Atacama Large Millimeter Array (ALMA)*, to probe the properties of the ISM of nearby ETGs and achieve a fuller understanding of the gas that drives the star formation in these galaxies at late epochs.**

ACKNOWLEDGEMENTS

SK acknowledges fellowships from the Royal Commission for the Exhibition of 1851, Imperial College London, Worcester College, Oxford and support from the BIPAC institute at Oxford. MB acknowledges support through STFC rolling grant PP/E001114/1. S. S. thanks the Australian Research Council and New College, Oxford for research fellowships.

REFERENCES

- Abazajian K. N., et al. 2009, *ApJS*, 182, 543
- Annibali F., Bressan A., Rampazzo R., Zeilinger W. W., Vega O., Panuzzo P., 2010, *A&A*, 519, A40+
- Baldwin J. A., Phillips M. M., Terlevich R., 1981, *PASP*, 93, 5
- Bell E. F., McIntosh D. H., Katz N., Weinberg M. D., 2003, *ApJS*, 149, 289
- Bell E. F., Wolf C., Meisenheimer K., et al. 2004, *ApJ*, 608, 752
- Bernardi M., Sheth R. K., Annis J., Burles S., Finkbeiner D. P., Lupton R. H., Schlegel D. J., SubbaRao M., et al. 2003, *AJ*, 125, 1882

- Bertola F., 1987, in P. T. de Zeeuw ed., *Structure and Dynamics of Elliptical Galaxies* Vol. 127 of IAU Symposium, Properties of elliptical galaxies with dust lanes. pp 135–144
- Binney J., Tremaine S., 1987, *Galactic dynamics*
- Blanton M. R., Brinkmann J., Csabai I., et al. 2003, *AJ*, 125, 2348
- Blanton M. R., Roweis S., 2007, *AJ*, 133, 734
- Bower R. G., Lucey J. R., Ellis R., 1992, *MNRAS*, 254, 589
- Bregman J. N., Hogg D. E., Roberts M. S., 1992, *ApJ*, 387, 484
- Calura F., Pipino A., Matteucci F., 2008, *A&A*, 479, 669
- Canizares C. R., Fabbiano G., Trinchieri G., 1987, *ApJ*, 312, 503
- Combes F., Young L. M., Bureau M., 2007, *MNRAS*, 377, 1795
- Crockett R. M., et al. 2011, *ApJ*, 727, 115
- Davis T. A., et al. 2011, *ArXiv e-prints*
- Draine B. T., Lee H. M., 1984, *ApJ*, 285, 89
- Draine B. T., Salpeter E. E., 1979a, *ApJ*, 231, 438
- Draine B. T., Salpeter E. E., 1979b, *ApJ*, 231, 77
- Dwek E., 1986, *ApJ*, 302, 363
- Dwek E., Rephaeli Y., Mather J. C., 1990, *ApJ*, 350, 104
- Ebneter K., Davis M., Djorgovski S., 1988, *AJ*, 95, 422
- Faber S. M., Gallagher J. S., 1976, *ApJ*, 204, 365
- Faber S. M., Tremaine S., Ajhar E. A., Byun Y., Dressler A., Gebhardt K., Grillmair C., Kormendy J., Lauer T. R., Richstone D., 1997, *AJ*, 114, 1771
- Faber S. M., Willmer C. N. A., Wolf C., et al. 2007, *ApJ*, 665, 265
- Ferreras I., Lisker T., Pasquali A., Khochfar S., Kaviraj S., 2009, *MNRAS*, 396, 1573
- Finkelman I., Brosch N., Kniazev A. Y., Buckley D. A. H., O’Donoghue D., Hashimoto Y., Loaring N., Romero-Colmenero E., Still M., Sefako R., Väisänen P., 2008, *MNRAS*, 390, 969
- Forbes D. A., 1991, *MNRAS*, 249, 779
- Forbes D. A., Ponman T. J., Brown R. J. N., 1998, *ApJ*, 508, L43
- Fukugita M., Nakamura O., Turner E. L., Helmboldt J., Nichol R. C., 2004, *ApJL*, 601, L127
- Gordon M. A., 1991, *ApJ*, 371, 563
- Goudfrooij P., de Jong T., 1995, *A&A*, 298, 784
- Goudfrooij P., de Jong T., Hansen L., Norgaard-Nielsen H. U., 1994a, *MNRAS*, 271, 833
- Goudfrooij P., de Jong T., Hansen L., Norgaard-Nielsen H. U., 1994b, *MNRAS*, 271, 833
- Hawarden T. G., Longmore A. J., Tritton S. B., Elson R. A. W., Corwin Jr. H. G., 1981, *MNRAS*, 196, 747
- Henkel C., Wiklind T., 1997, *SSRv*, 81, 1
- Hildebrand R. H., 1983, *QJRAS*, 24, 267
- Jeong H., et al. 2009, *MNRAS*, 398, 2028
- Jeong H., Bureau M., Yi S. K., Krajnović D., Davies R. L., 2007, *MNRAS*, 376, 1021
- Jogee S., Miller S. H., Penner K., et al. 2009, *ApJ*, 697, 1971
- Jorgensen I., Franx M., Kjaergaard P., 1996, *MNRAS*, 280, 167
- Kauffmann G., Heckman T. M., White S. D. M., et al. 2003, *MNRAS*, 346, 1055
- Kaviraj S., et al. 2007, *ApJS*, 173, 619
- Kaviraj S., 2010, *MNRAS*, 408, 170
- Kaviraj S., Khochfar S., Schawinski K., et al. 2008, *MNRAS*, 388, 67
- Kaviraj S., Peirani S., Khochfar S., Silk J., Kay S., 2009, *MNRAS*, 394, 1713
- Kaviraj S., Tan K.-M., Ellis R. S., Silk J., 2011, *MNRAS*, 411, 2148
- Kewley L. J., Groves B., Kauffmann G., Heckman T., 2006, *MNRAS*, 372, 961
- Knapp G. R., 1999, in P. Carral & J. Cepa ed., *Star Formation in Early Type Galaxies* Vol. 163 of *Astronomical Society of the Pacific Conference Series*, Cold Gas and Star Formation in Elliptical Galaxies. pp 119–+
- Knapp G. R., Guhathakurta P., Kim D., Jura M. A., 1989, *ApJS*, 70, 329
- Knapp G. R., Gunn J. E., Wynn-Williams C. G., 1992, *ApJ*, 399, 76
- Knapp G. R., Rupen M. P., 1996, *ApJ*, 460, 271
- Krumholz M. R., McKee C. F., 2005, *ApJ*, 630, 250
- Kwan J., Xie S., 1992, *ApJ*, 398, 105
- Lees J. F., Knapp G. R., Rupen M. P., Phillips T. G., 1991, *ApJ*, 379, 177
- Leroy A. K., et al. 2008, *AJ*, 136, 2782
- Lintott C., Schawinski K., Bamford S., et al. 2010, *ArXiv e-prints*
- Lintott C. J., Schawinski K., Slosar A., et al. 2008, *MNRAS*, 389, 1179
- López-Sanjuan C., Balcells M., Pérez-González P. G., Barro G., Gallego J., Zamorano J., 2010, *ArXiv e-prints*
- Martin D. C., Fanson J., Schiminovich D., et al. 2005, *ApJ*, 619, L1
- Martin J. R., O’Connell R. W., Hibbard J. E., 2009, in M. Chávez Dagostino, E. Bertone, D. Rosa Gonzalez, & L. H. Rodríguez-Merino ed., *New Quests in Stellar Astrophysics. II. Ultraviolet Properties of Evolved Stellar Populations Near-UV Merger Signatures in Early-Type Galaxies*. pp 83–88
- Mathews W. G., Brighenti F., 2003, *AR&A*, 41, 191
- Merluzzi P., 1998, *A&A*, 338, 807
- Miller C. J., Nichol R. C., Gómez P. L., Hopkins A. M., Bernardi M., 2003, *ApJ*, 597, 142
- Morrissey P., et al. 2007, *ApJS*, 173, 682
- Mulchaey J. S., Jeltema T. E., 2010, *ApJL*, 715, L1
- Peirani S., Crockett R. M., Geen S., Khochfar S., Kaviraj S., Silk J., 2010, *MNRAS*, 405, 2327
- Rodgers C. T., Canterna R., Smith J. A., Pierce M. J., Tucker D. L., 2006, *AJ*, 132, 989
- Rowan-Robinson M., 1986, *MNRAS*, 219, 737
- Sadler E. M., Gerhard O. E., 1985, 214, 177
- Sage L. J., Galletta G., 1993, *ApJ*, 419, 544
- Saglia R. P., Colless M., Baggley G., et al. 1997, in Arnaboldi M., Da Costa G. S., Saha P., eds, *ASP Conf. Ser. 116: The Nature of Elliptical Galaxies; 2nd Stromlo Symposium The EFAR Fundamental Plane*. pp 180–+
- Sahu D. K., Pandey S. K., Kembhavi A., 1998, *A&A*, 333, 803
- Salim S., Rich R. M., 2010, *ApJ*, 714, L290
- Sarzi M., Falcón-Barroso J., Davies R. L., et al. 2006, *MNRAS*, 366, 1151
- Sarzi M., Shields J. C., Schawinski K., et al. 2010, *MNRAS*, 402, 2187
- Schawinski K., Thomas D., Sarzi M., Maraston C., Kaviraj S., Joo S., Yi S. K., Silk J., 2007, *MNRAS*, 382, 1415

- Schaye J., 2004, *ApJ*, 609, 667
Schwartz P. R., 1982, *ApJ*, 252, 589
Schweizer F., Seitzer P., 1992, *AJ*, 104, 1039
Schweizer F., Seitzer P., Faber S. M., Burstein D., Dalle Ore C. M., Gonzalez J. J., 1990, *ApJ*, 364, L33
Spitzer L., 1978, *Physical processes in the interstellar medium*
Stewart K. R., Bullock J. S., Wechsler R. H., Maller A. H., Zentner A. R., 2008, *ApJ*, 683, 597
Stoughton C., et al. 2002, *AJ*, 123, 485
Suh H., Jeong H., Oh K., Yi S. K., Ferreras I., Schawinski K., 2010, *ApJS*, 187, 374
Thomas D., Greggio L., Bender R., 1999, *MNRAS*, 302, 537
Thronson Jr. H. A., Tacconi L., Kenney J., Greenhouse M. A., Margulis M., Tacconi-Garman L., Young J. S., 1989, *ApJ*, 344, 747
Tomita A., Aoki K., Watanabe M., Takata T., Ichikawa S.-i., 2000, *AJ*, 120, 123
Trager S. C., Faber S. M., Worthey G., González J. J., 2000a, *AJ*, 119, 1645
Trager S. C., Faber S. M., Worthey G., González J. J., 2000b, *AJ*, 120, 165
Tran H. D., Tsvetanov Z., Ford H. C., Davies J., Jaffe W., van den Bosch F. C., Rest A., 2001, *AJ*, 121, 2928
Tubbs A. D., 1980, *ApJ*, 241, 969
van Dokkum P. G., Franx M., 1995, *AJ*, 110, 2027
van Dokkum P. G., Franx M., 1996, *MNRAS*, 281, 985
Vanden Berk D. E., et al. 2001, *AJ*, 122, 549
Veilleux S., Osterbrock D. E., 1987, *ApJS*, 63, 295
Wang L., Rowan-Robinson M., 2009, *MNRAS*, 398, 109
Wang Z., Kenney J. D. P., Ishizuki S., 1992, *AJ*, 104, 2097
Whitaker K. E., van Dokkum P. G., 2008, *ApJL*, 676, L105
Wiklind T., Henkel C., 1989, *A&A*, 225, 1
Wiklind T., Henkel C., 1995, *A&A*, 297, L71+
Wong T., Blitz L., 2002, *ApJ*, 569, 157
Yang X., Mo H. J., van den Bosch F. C., 2008, *ApJ*, 676, 248
Yang X., Mo H. J., van den Bosch F. C., Pasquali A., Li C., Barden M., 2007, *ApJ*, 671, 153
Yi S. K., Yoon S.-J., Kaviraj S., et al. 2005, *ApJ*, 619, L111
York D. G., SDSS collaboration 2000, *AJ*, 120, 1579
Young J. S., Xie S., Kenney J. D. P., Rice W. L., 1989, *ApJS*, 70, 699
Young L. M., et al. 2011, arXiv:1102.4633
Zeilinger W. W., Bertola F., Galletta G., 1990, in E. Bussoletti & A. A. Vittone ed., *Dusty Objects in the Universe* Vol. 165 of *Astrophysics and Space Science Library*, *Elliptical Galaxies with Dust Lanes*. pp 227–+